CLIMATE CHANGE INFLUENCE CARBON CYCLE STUDY ON WETLANDS IN POLAND

Katarzyna Dabrowska– Zielinska; Radoslaw Gurdak; Patryk Grzybowski; Maciej Bartold; Marcin Kluczek, Dariusz Ziółkowski

katarzyna.dabrowska-zielinska@igik.edu.pl

Institute of Geodesy and Cartography – Remote Sensing Center

Warszawa – Modzelewskiego 27 Poland

The work has been funded by the National project - Narodowe Centrum Nauki 2016/23/B/ST10/03155.

www.igik.edu.pl

Global annual near surface temperature has been rising steadily since the end of the 19th century. The rate of increase has been particularly high **since the 1970s** at about 0.2°C per decade.

Anthropogenic activities, particularly **greenhouse gas (GHG) emissions, are largely responsible for this warming**.
To prevent serious environmental, economic and societal impacts of climate change, all signatories to the United Nations Framework Convention on Climate Change (UNFCCC) committed in the 2015 Paris Agreement to limiting global temperature increase to well below 2°C above pre-industrial levels by 2050 and to pursuing efforts to limit the increase to 1.5°C

Europe is warming faster than the global average. The mean annual temperature over European land areas in the last decade was 1.94 to 2.01°C warmer than during the pre-industrial period. The year 2020 was the warmest year in Europe since the instrumental records began according to all datasets used, with the range of anomaly between 2.51°C and 2.74°C above the pre-industrial levels. Particularly high warming has been observed over eastern Europe, Scandinavia and at eastern part of Iberian Peninsula.
Projections from the World Climate Programme initiative suggest that temperatures across European land areas will continue to increase throughout this century at a higher rate than the global average. Land temperatures in Europe are projected to increase further by 1.2 to 3.4°

Greenhouse gases emitted by human activities alter Earth's energy balance and thus its climate. Humans also affect climate by changing the nature of the land surfaces (for example by clearing forests for farming) and through the emission of pollutants that affect the amount and type of particles in the atmosphere.

Greenhouse gases affect Earth's energy balance and climate

The Sun serves as the primary energy source for Earth's climate. Some of the incoming sunlight is reflected directly back into space, especially by bright surfaces such as ice and clouds, and the rest is absorbed by the surface and the atmosphere. **Much of this absorbed solar energy is re-emitted as heat** (longwave or infrared radiation). The atmosphere in turn absorbs and re-radiates heat, some of which escapes to space. Any disturbance to this balance of incoming and outgoing energy will affect the climate. For example, small changes in the output of energy from the Sun will affect this balance directly.

Scientists have determined that, when all human and natural factors are considered, Earth's climate balance has been altered towards warming, with the biggest contributor being increases in CO_2.

Warming leads to further effects (feedbacks) that either amplify or diminish the initial warming.

The most important feedbacks involve various forms of water. A warmer atmosphere generally contains more water vapour. Water vapour is a potent greenhouse gas, thus causing more warming; Thus, water vapour is treated as an amplifier, and not a driver, of climate change. Higher temperatures in the polar regions melt sea ice and reduce seasonal snow cover, exposing a darker ocean and land surface that can absorb more heat, causing further warming. Another important but uncertain feedback concerns changes in clouds. Warming and increases in water vapour together may cause cloud cover to increase or decrease which can either amplify or dampen temperature change depending on the changes in the horizontal extent, altitude, and properties of clouds. The latest assessment of the science indicates that the overall net global effect of cloud changes is likely to be to amplify warming.

Taken together, all model projections indicate that Earth will continue to warm considerably more over the next few decades to centuries. If there were no technological or policy changes to reduce emission trends from their current trajectory, then further globally-averaged warming of 2.6 to 4.8 °C in addition to that which has already occurred would be expected during the 21st century. Projecting what those ranges will mean for the climate experienced at any particular location is a challenging scientific problem, but estimates are continuing to improve as regional and local-scale models advance.

The highest level of warming is projected across north-eastern Europe, northern Scandinavia and inland areas of Mediterranean countries, while the lowest warming is expected in western Europe, especially in the United Kingdom, Ireland, western France, Benelux countries and Denmark.

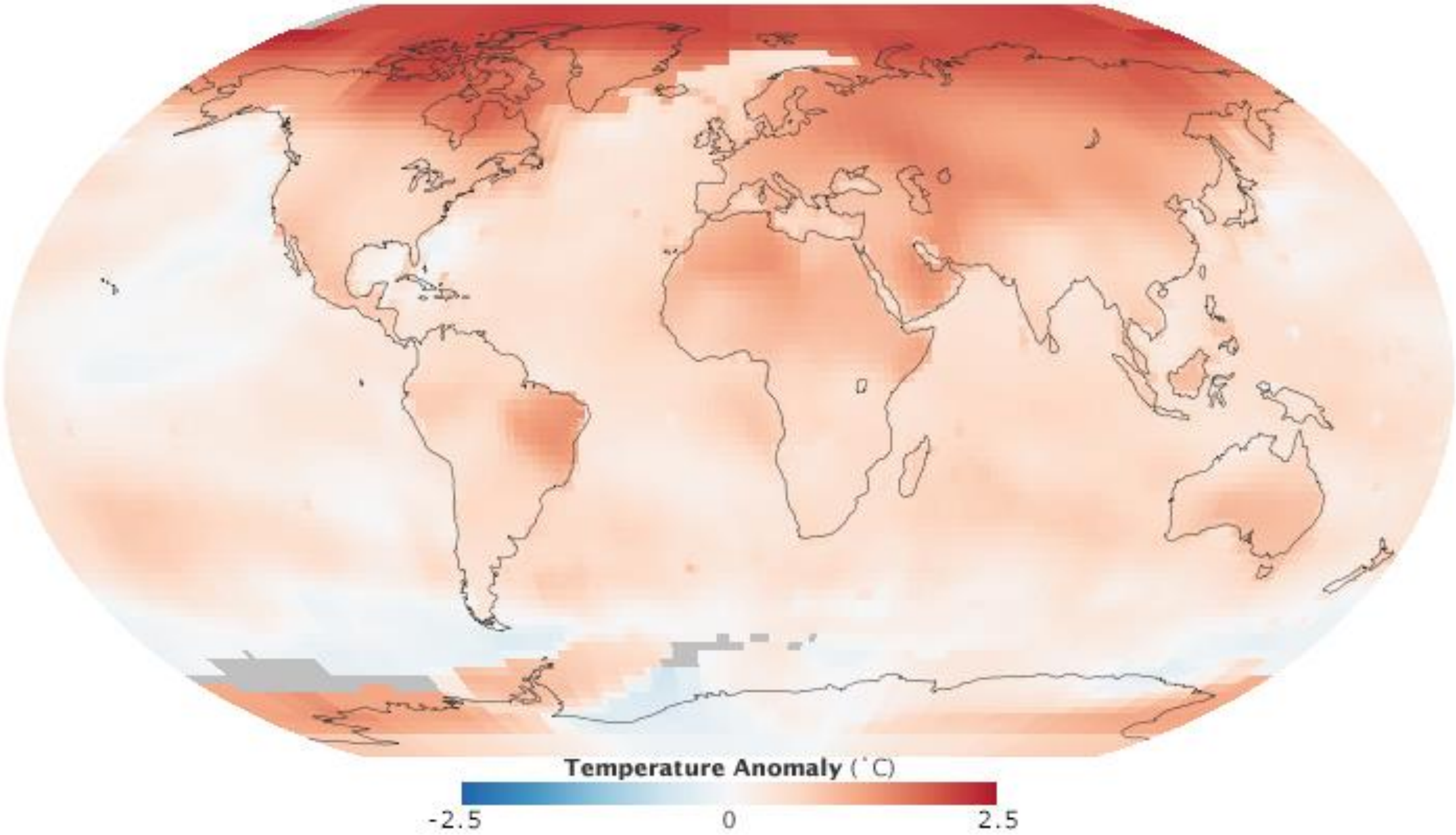
Temperature Anomaly (˚C)
-2.5
0
2.5

Effect of the Drought River bed – Poland

Fot. Adobe Stock Zdjecie rzeki

Balkans lake dried up 2022

Fot Jan Krynski

Flood – Indus River Pakistan 2022 -In the provinces of Sindh and Balochistan, rainfall exceeded the average by 500 percent, devouring entire villages and farmlands and destroying buildings

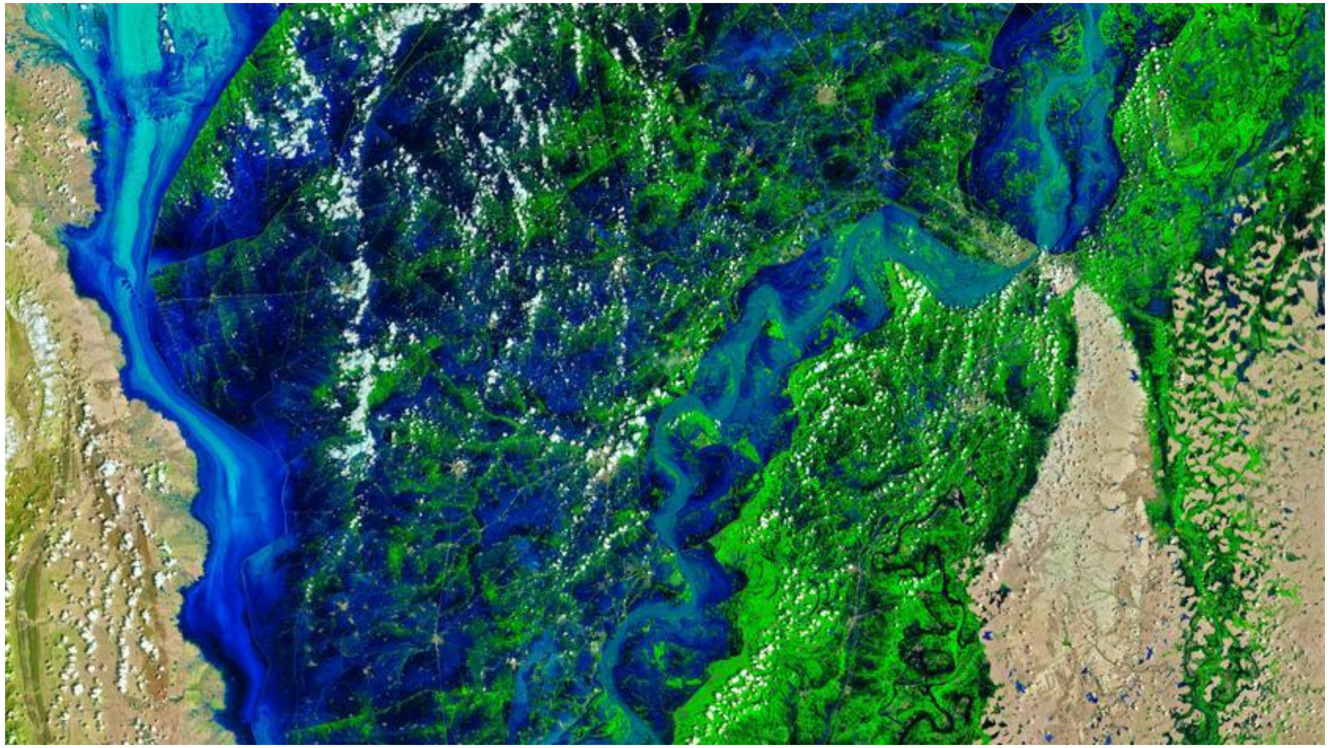

Indus River. 28.08.2022earthobservatory.nasa.gov

Zdjęcie z dnia 4.08.2022
According to earthobservatory.nasa.gov

New types of crop due to the increase of temperaturę

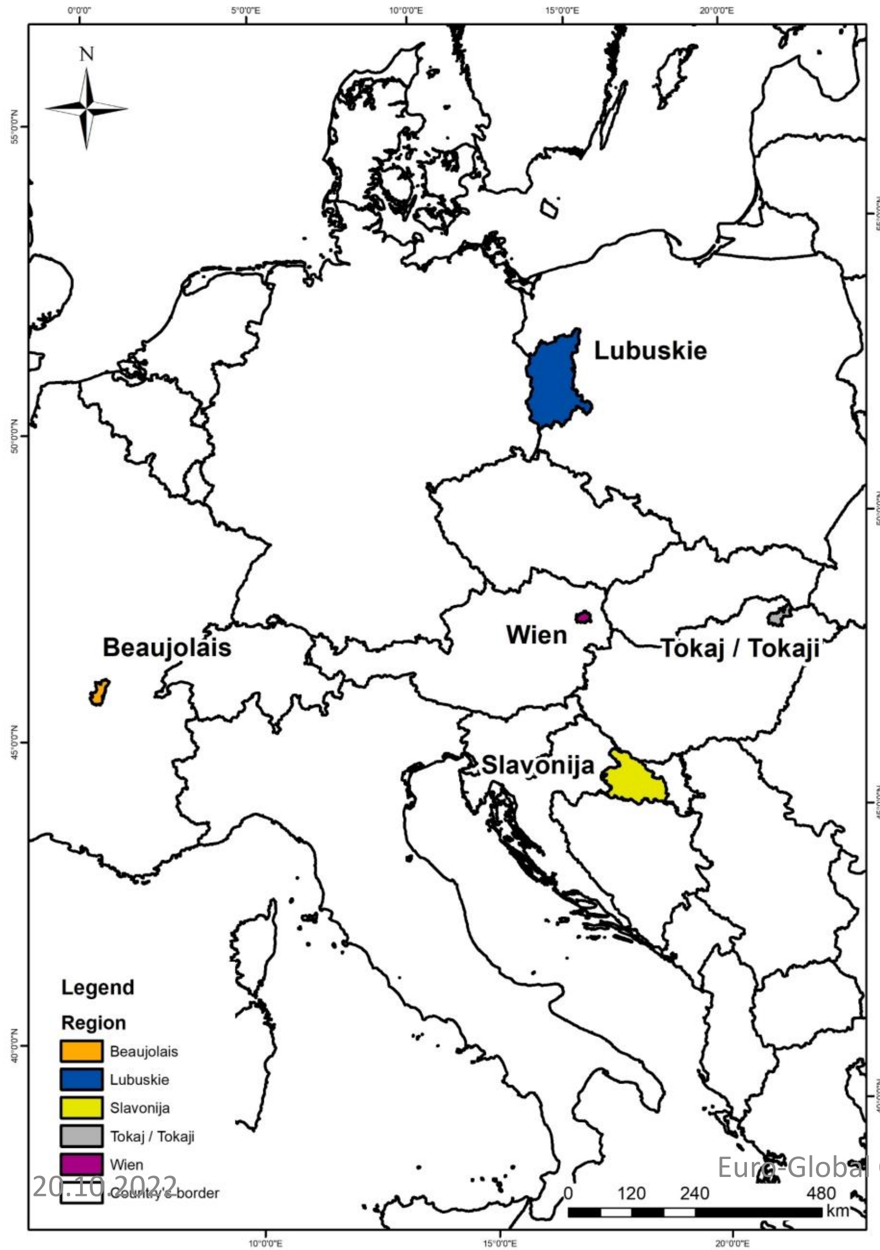

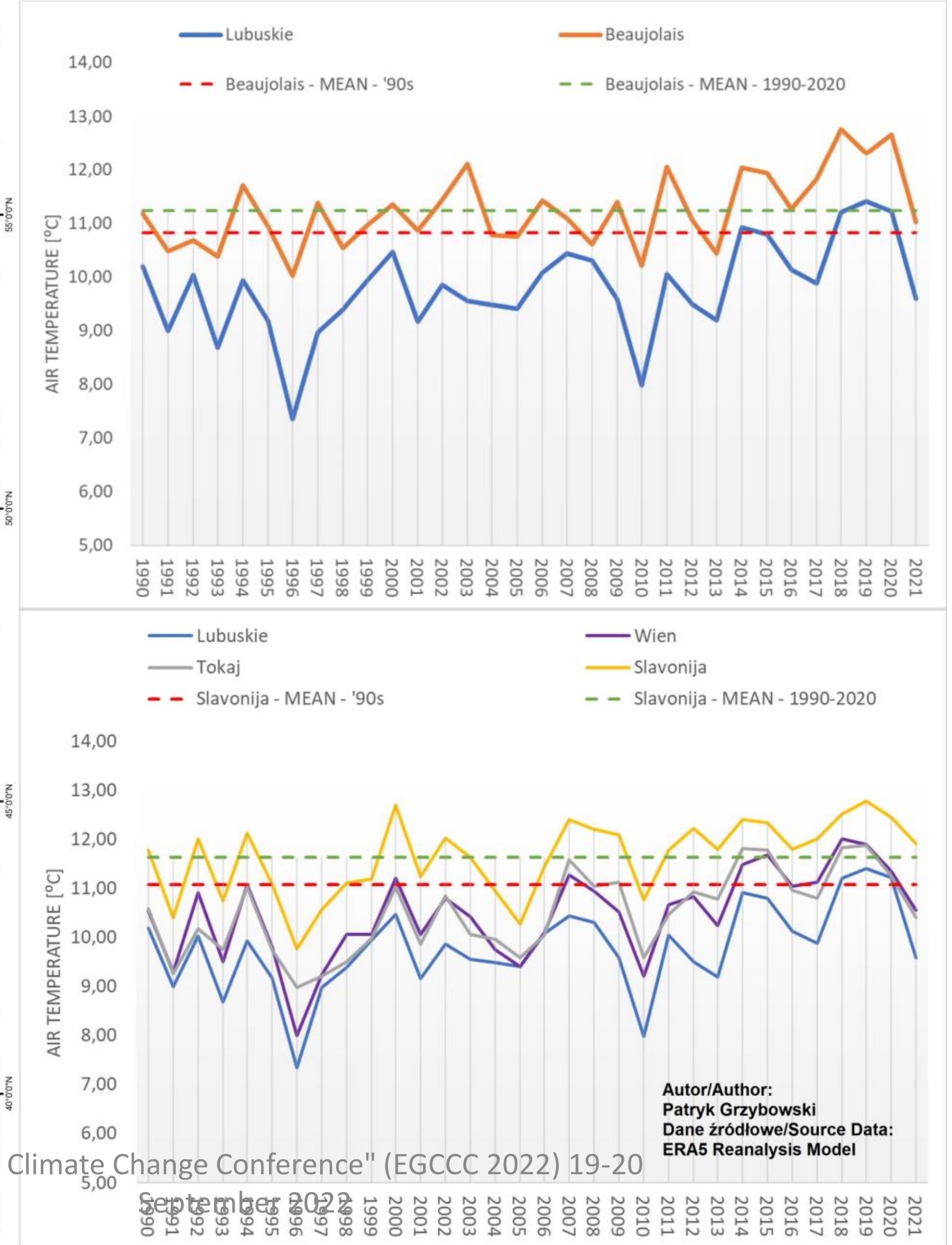

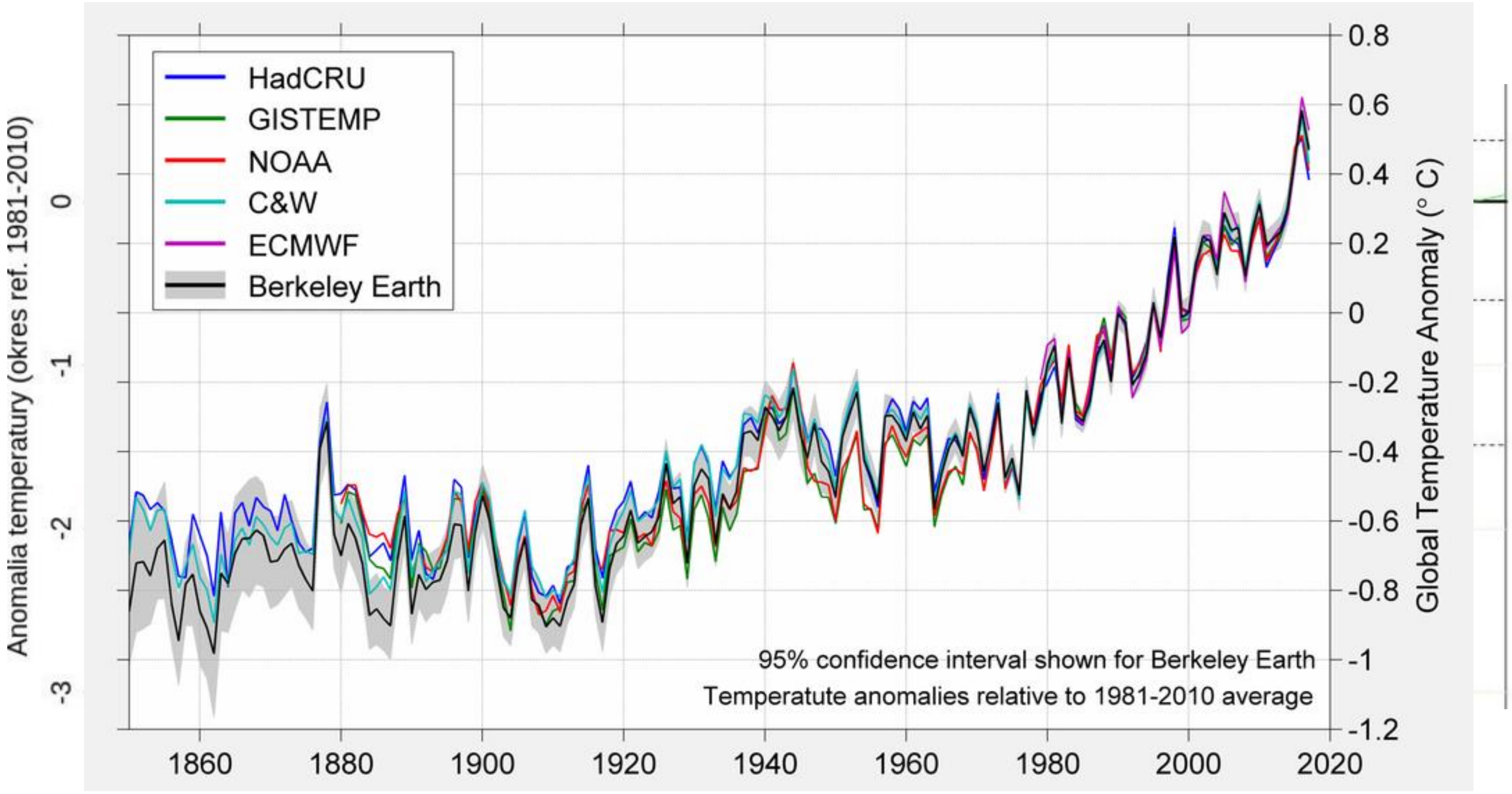

HadCRU
GISTEMP
NOAA
C&W
ECMWF
Berkeley Earth
95% confidence interval shown for Berkeley Earth
Temperatute anomalies relative to 1981-2010 average
Anomalia temperatury (okres ref. 1981-2010)
Global Temperature Anomaly (° C)
0
-1
-2
-3
0.8
0.6
0.4
0.2
0
-0.2
-0.4
-0.6
-0.8
-1
-1.2
1860
1880
1900
1920
1940
1960
1980
2000
2020

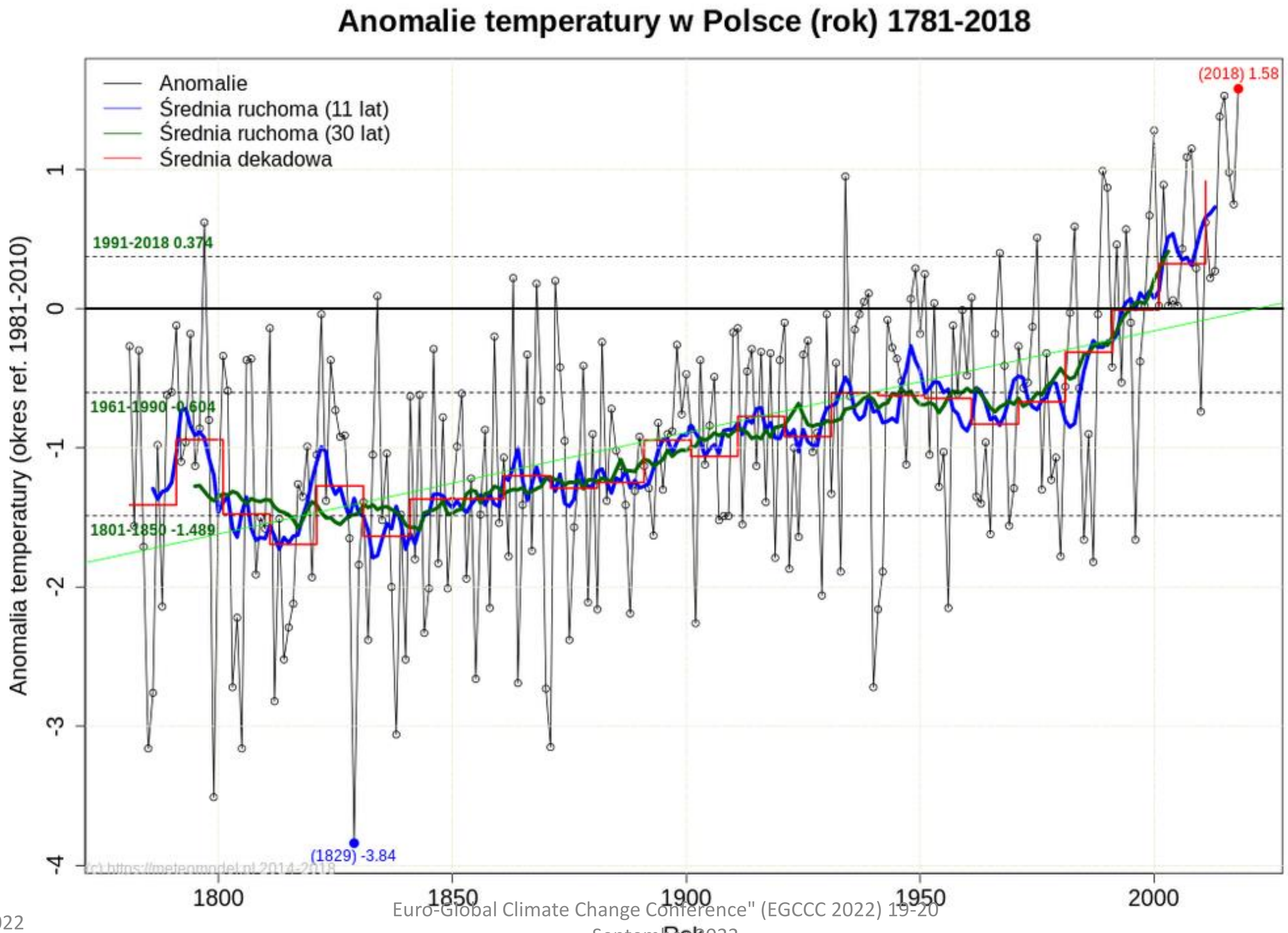
Anomalie temperatury w Polsce (rok) 1781-2018
Anomalie
Średnia ruchoma (11 lat)
Średnia ruchoma (30 lat)
Średnia dekadowa
(2018) 1.58
1991-2018 0.374
1961-1990 -0.604
1801-1850 -1.489
(1829) -3.84
Anomalia temperatury (okres ref. 1981-2010)
1
0
-1
-2
-3
-4
1800
1850
1900
1950
2000
Rok

Air Polution 2004-2021PM2.5 in Europe

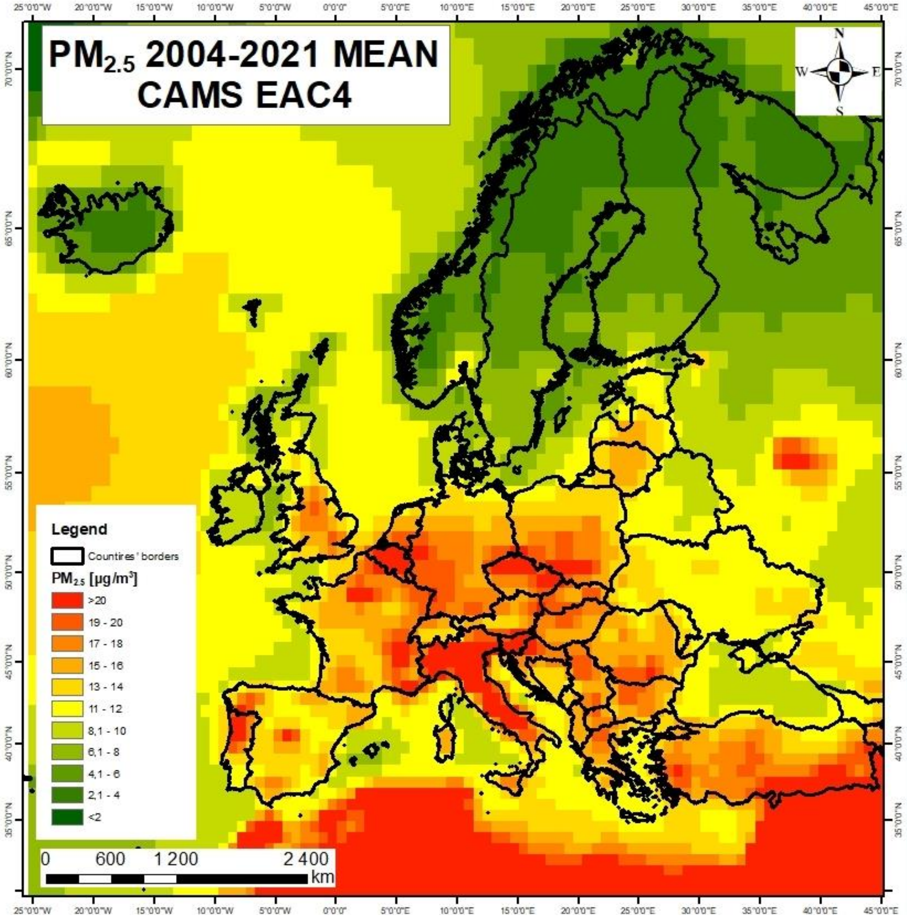

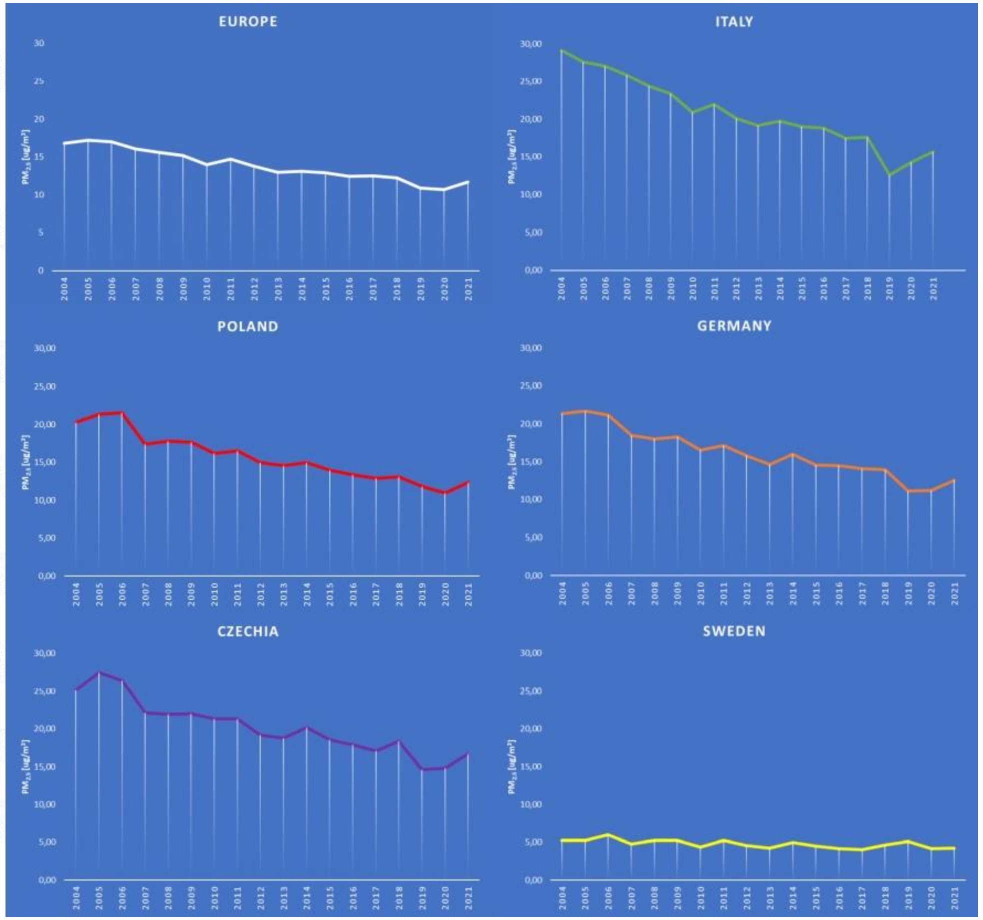

TERRA.MODIS OBSERVATIONS OF SNOW COVER OVER POLAND
COMPARISON BETWEEN YEARS 2019 - 2022

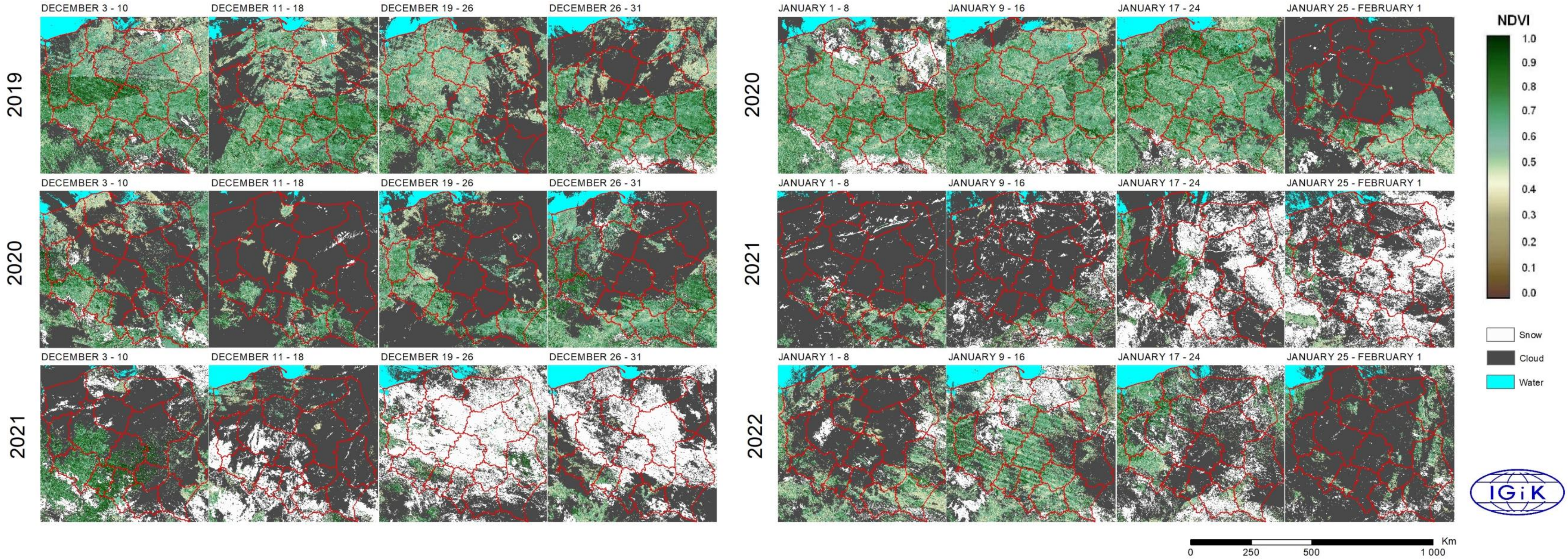

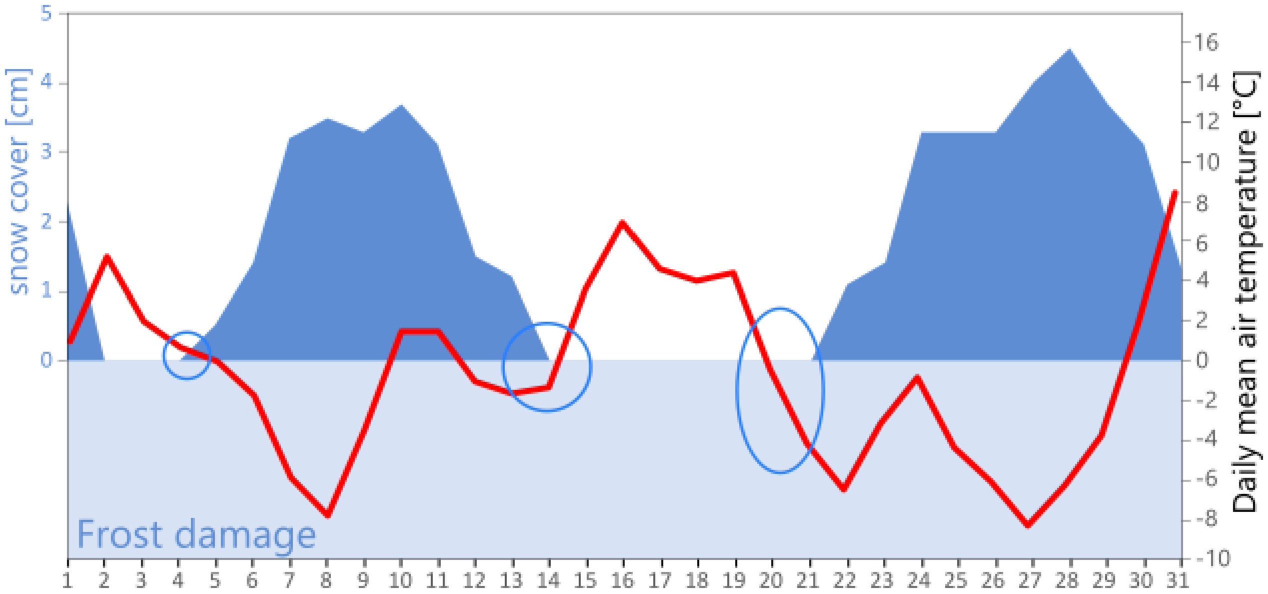
snow cover [cm]
Daily mean air temperature [°C]
Frost damage

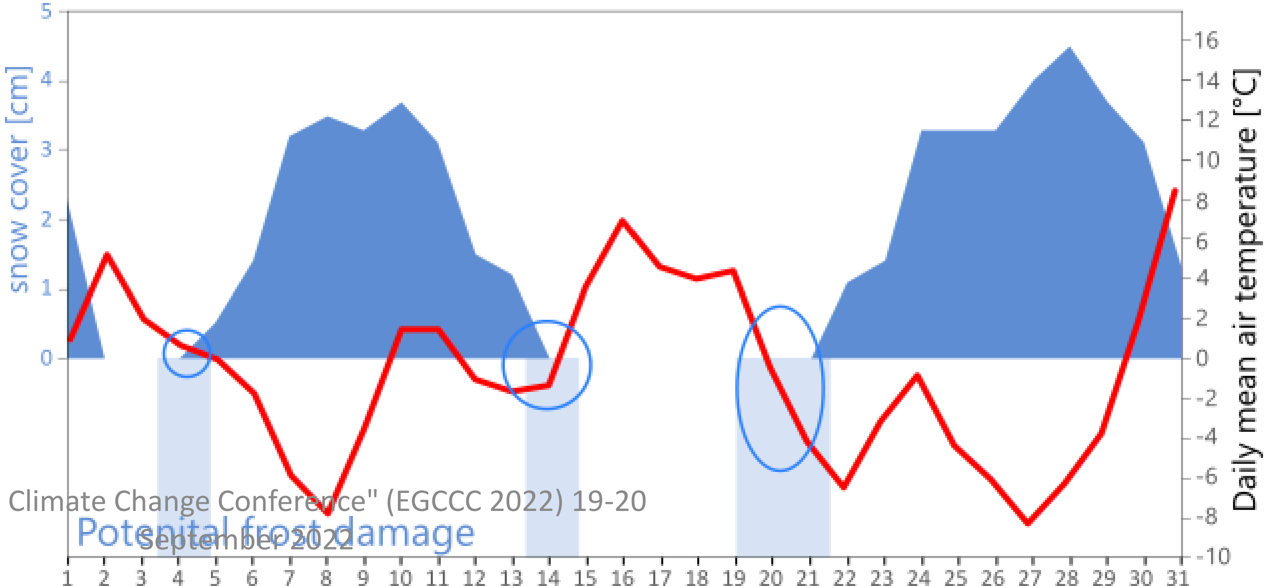
snow cover [cm]
Daily mean air temperature [°C]
Potenital frost damage

Agricultural drought hazard indices applied for drought identification

Selyaninov's Hydrothermal Coefficient - HTC

$$HTC = \frac{10 \sum_{i=1}^{n} P_i}{\sum_{i=1}^{n} T_i}$$

where:
n – number of days preceding the analyzed date;
Pi – precipitation value at ***i*** day (mm);
Ti – mean daily temperature at ***i*** day(°C)

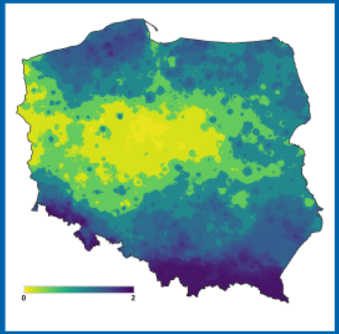

HTC MEDIAN (1997-2018)

Temperature Condition Index - TCI

$$TCI = \frac{(Ts\_max - Ts)}{(Ts\_max - Ts\_min)} * 100$$

where:
Ts – value of surface radiation temperature from the current ten-day period;
Ts_max – maximum value of surface radiation temperature from 1997 – 2018 period;
Ts_min - minimum value of surface radiation temperature from 1997 – 2018 period

There is the logarithmic relationship between cumulation of precipitation vs. air temperature (HTC) and satellite radiation temperature

$$\ln(HTC) \approx f(TCI)$$

Satellite index of agricultural drought identification

$$DISS_d = M_{HTC} * \exp(A * TCI_d + B * TCI_{d-1} + C * TCI_{d-2})$$

where:
M_HTC - HTC median; TCI – Temperature Condition Index
d – ten-day period (12 – 27);
A, B, C – estimated parameters for moving average TCI *d* TCI *d-1* TCI *d-2*

The maps present the areas where the thermal conditions for vegetation are average (light green), very good (green) dry (orange) or extreme dry (red color). Additionally, the blue color means the wet conditions.

10-day period (AUGUST 11-20) 2015 | AUGUST 21-30 2015 | SEPTEMBER 1-10 2015

HTC

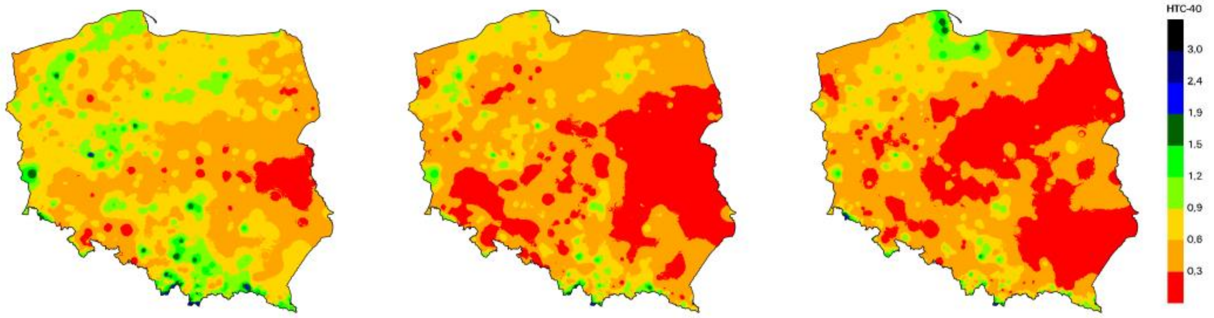

TCI

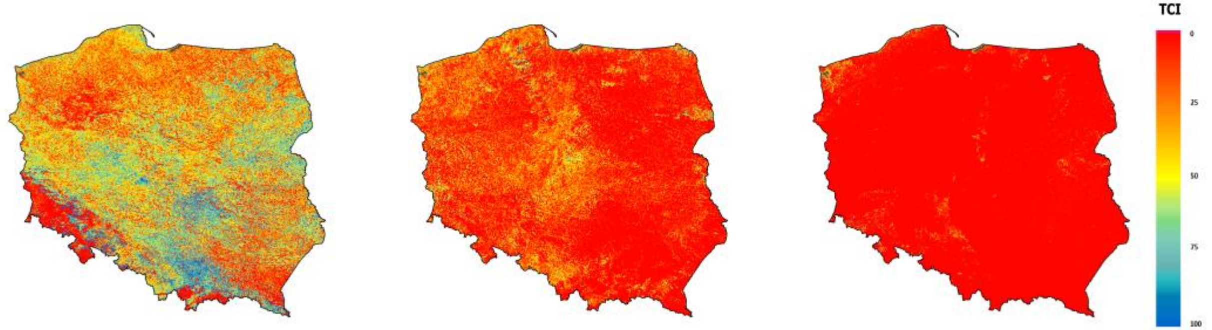

DISS

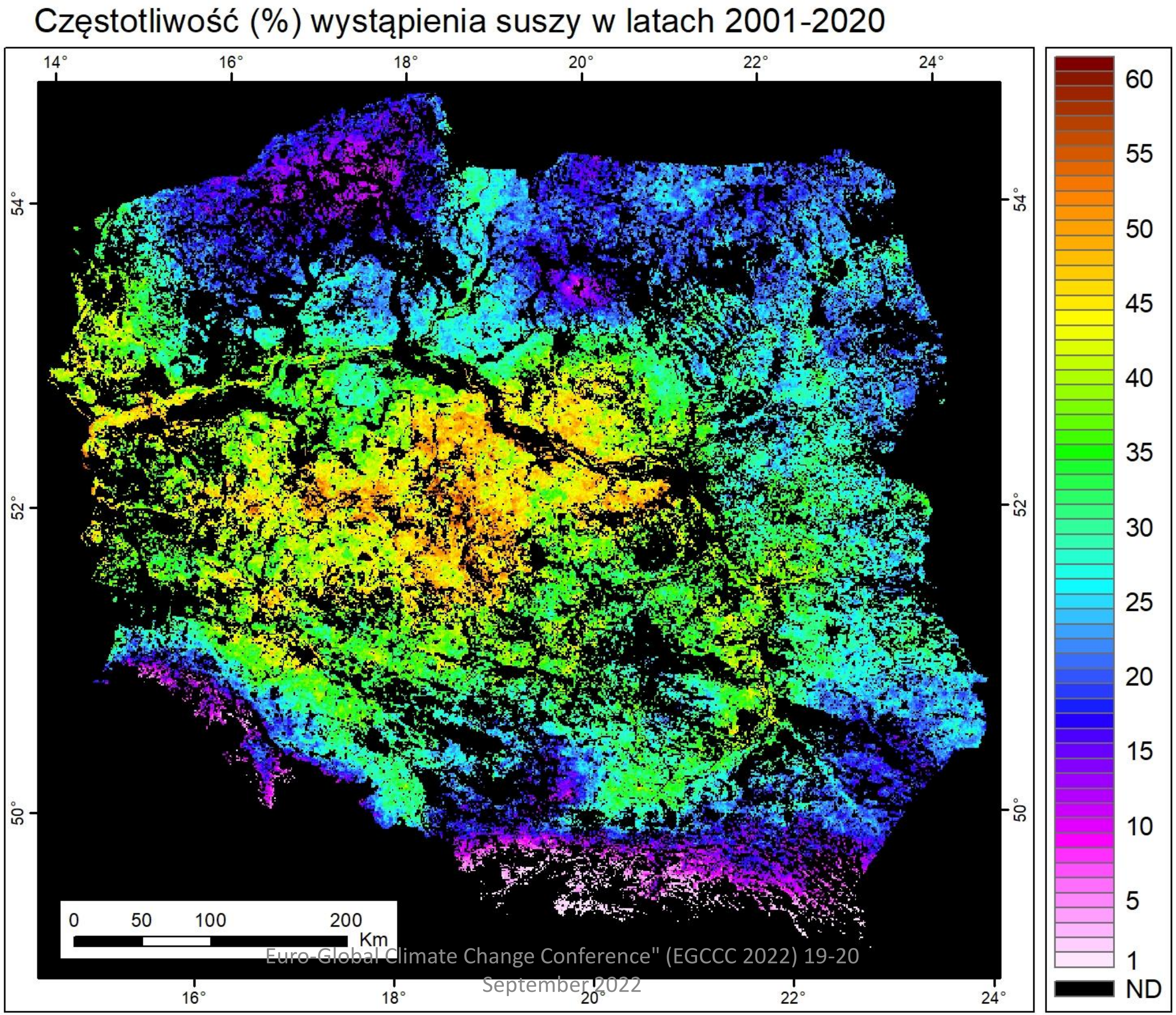
Częstotliwość (%) wystąpienia suszy w latach 2001-2020
14°
16°
18°
20°
22°
24°
54°
52°
50°
0
50
100
200
Km
60
55
50
45
40
35
30
25
20
15
10
5
1
ND

Surface deformation in Semarang City in the new build areas - Jratunseluna watershed Level of underground water (Central Java – Indonesia)

climate change. the recession of the shoreline inland occurs in the area of the strongest deformation (intense purple color). Therefore,, this can be treated as direct human impact on local changes in the coastline,

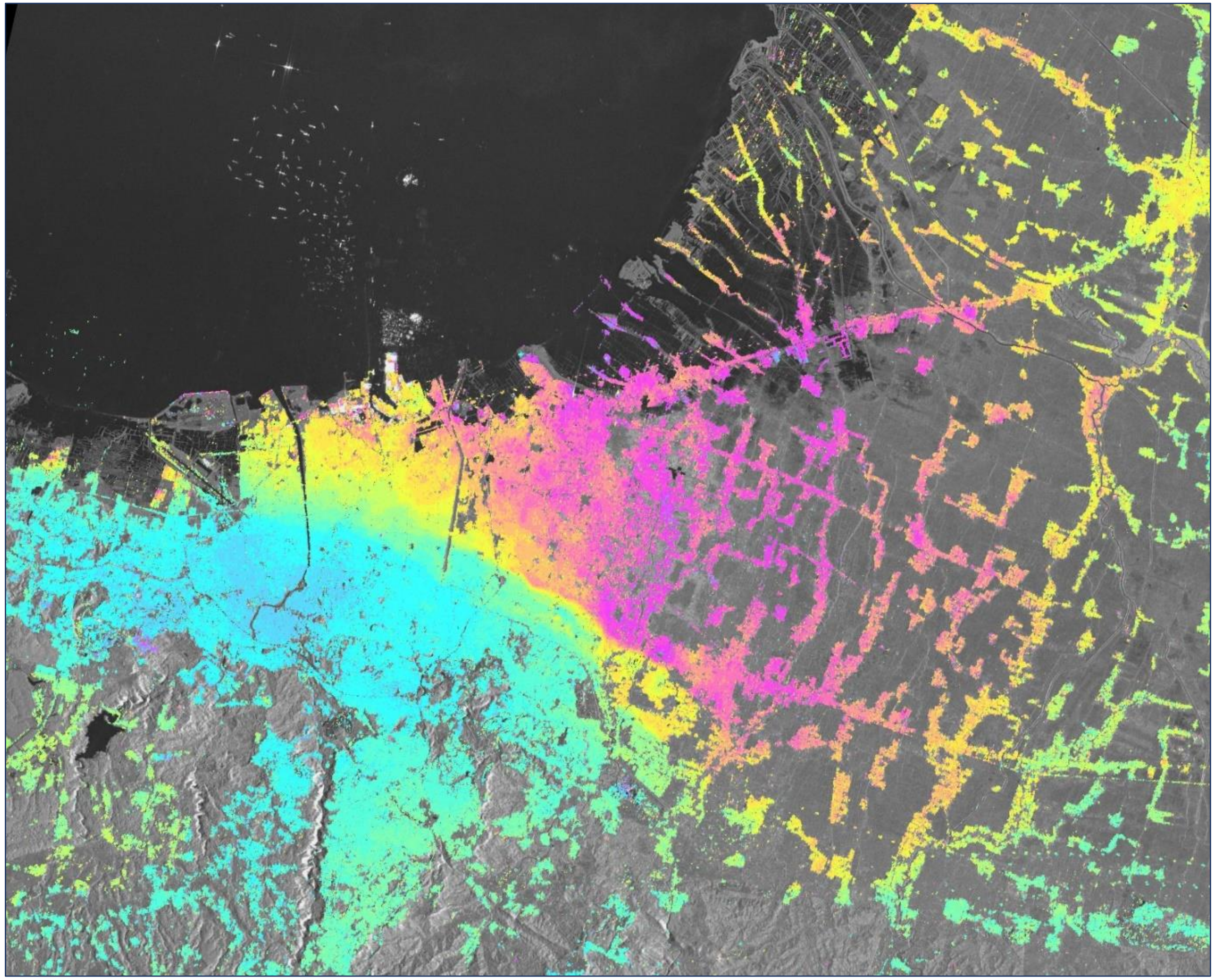

The deformation map of the part of Jratunseluna watershed (Semarang City and surroundings) based on the Sentinel-1 data registered from January 2017 to January 2018 from descending orbit D76.

Land subsidence is mainly caused by the increased extraction of groundwater resulting from the development of urban areas and rapid population growth

Plants use energy from light to convert water and carbon dioxide into sugar and oxygen in a process called photosynthesis.
Forests act as carbon "sinks" and reduce the amount of carbon dioxide in the air significantly.

The United Nations, through its Intergovernmental Panel on Climate Changes and UN-REDD -- Reducing Emissions from Deforestation and forest Degradation -- program, works to discourage deforestation in developing countries. The REDD+ program provides financial incentives for developing countries to reduce deforestation by assigning financial value to forests’ carbon-storage capabilities.

GPP, the amount of Carbon fixed by terrestrial ecosystems through photosynthesis, constitutes the largest Carbon flux between the terrestrial biosphere and the atmosphere.

A part of the Carbon absorbed is returned to the atmosphere through plant respiration and the difference between GPP and autotrophic respiration is termed as Net Primary Production - NPP.

Disturbances as drought are critical ecosystem processes that influence Carbon cycle dynamics.

Direct emissions from one disturbance type, **wildfire,** transfer Carbon from ecosystems to the atmosphere immediately These impacts can last for decades as ecosystems recover.

Better understanding the terrestrial Carbon cycle has important implications for the climate

Remote sensing (optical and radars) plays the important role in quantifying Carbon fluxes quantified with remotely sensed data acquired in the broad wavelength range

Jingfeng Xiaoet al2019 Remote Sensing of the terrestrial carbon cycle

Remote sensing of the terrestrial Carbon cycle started from the launch of the first Landsat satellite (Landsat 1) on July 23, 1972. From Landsat 1 to Landsat 8) (US NASA)
satellites (Landsat 1–8), co-managed by U.S. Geological Survey (USGS) and National Aeronautics and Space Administration
(NASA), provides the longest continuous observations of the Earth's surface from space (Wulder et al., 2016). Imagery from the Landsat series of satellites (Landsat 1–8) has been used to quantify C fluxes and
stocks at regional to global scales (Foody et al., 2003; Masek and Collatz, 2006). The Landsat archive now includes almost 50 years of observations globally, providing opportunities for investigating regional
or global ecosystem C dynamics at multidecadal scales.
The most widely used AVHRR-derived NDVI records are perhaps the Global Inventory Monitoring and Modeling Studies (GIMMS) NDVI dataset and the GIMMS3g product

The MODerate resolution Imaging Spectroradiometer (MODIS) on board two key satellites of NASA's Earth Observing System (EOS) -Terra and Aqua provides observations of the Earth's surface and atmosphere with daily coverage in 36 spectral bands and a spatial resolution from 250m to 1 km

Jingfeng Xiaoet al2019 Remote Sensing of the terrestrial carbon cycle

The heatwave that swept through Western Europe in July 2022 put a historic heat record in Britain.
In the English county of Lincolnshire, 40.3 degrees Celsius has been recorded.
For the first time in history in the UK, the temperature measured in the shade exceeded 40 degrees.

As we notice, the grass has died back to nothing.

Biebrza wetlands - unique in Europe

- one of the largest area in Europe covered with marshes, swamps, and wet meadows
- 60 000 ha of flat river valley covered with hydrogenic soils such as peat in various stages of mouldering.
- habitat of 271 bird species
- protected as a National Park, Natura 2000 and RAMSAR sites

Unique environment of the Biebrza wetlands has to be preserved and constantly monitored. In this respect satellite observations in optical and radar bands have been utilized by the Remote Sensing Centre of IGiK for the last 15 years.

A variety of remotely sensed datasets as NDVI, LAI, FAPAR, LST has been used for the Wetlands Gross Primary Production – GPP have been used in the approache for the upscaling of Carbon fluxes. The remote sensing data have been used from MODIS ,Sentinel 2 and Sentinel 1 to estimate spatial GPP data.

We modelled the Gross Primary Production - GPP values using satellite derived parameters from Sentinel 2 , Sentinel 3 and MODIS data. There was a strong contribution of *NDVI*, *NDII*, *APAR*, evapotranspiration and the differences of LST and air temperature to the models.

The models presented as a result of this research can be used applying solely the satellite data The results of the analysis revealed that **NDVI index** is the driving factor for the assessment, of **GPP** independently on the type of satellite data.

The best fit has been achieved for the **Sentinel-3** models with inclusion of the other environmental parameters, as temperature difference **(**$T_s - T_a$**)** enhances model performance, Examination of peatland Biebrza in Poland . Peatlands and organic soils cover 3-5% of the world's land area and contain 30% of its soil carbon. Land vegetation is a key component in global climate cycles through its capacity for carbon (C) sequestration.

Peatlands on the one hand sequester the "greenhouse" gas from the atmosphere, while on the other hand they emit in large quantities both CO_2 and CH_4

In the boreal biome, forests cover ~ 8% of the land area and sequester approximately 272 ± 23 Gt of carbon, while northern peatlands store an estimated 415 ± 150 Gt of carbon, covering much less of the global land surface.

Degradation of peatlands is a growing source of anthropogenic GHG emissions.

Carbon dioxide emissions from peatland drainage, fires and exploitation are estimated to be the equivalent to at least 3,000 million tons per year. Climate changes induce decrease of precipitation and growth of air temperature what influences the exchange of the gases between the surface and atmosphere and lowers the soil moisture, what results in release of CO_2 to the atmosphere.

NPP – Net Primary Production

GPP versus NDVI

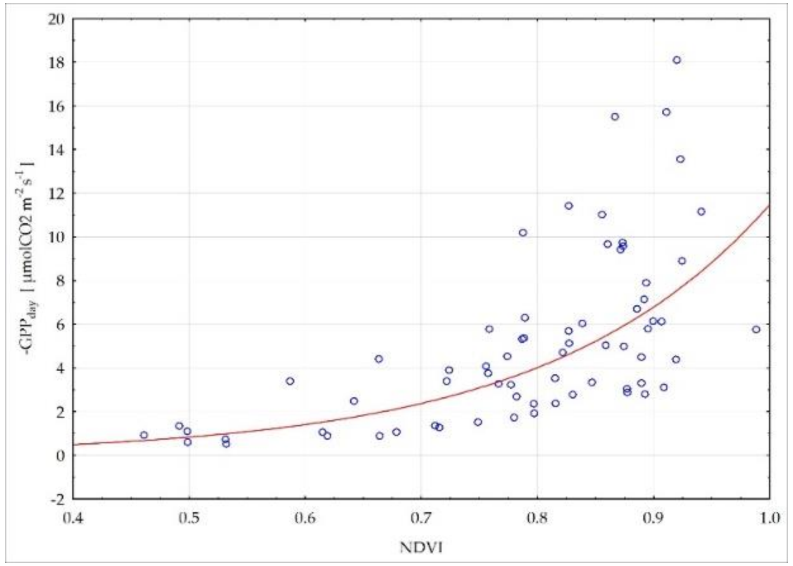

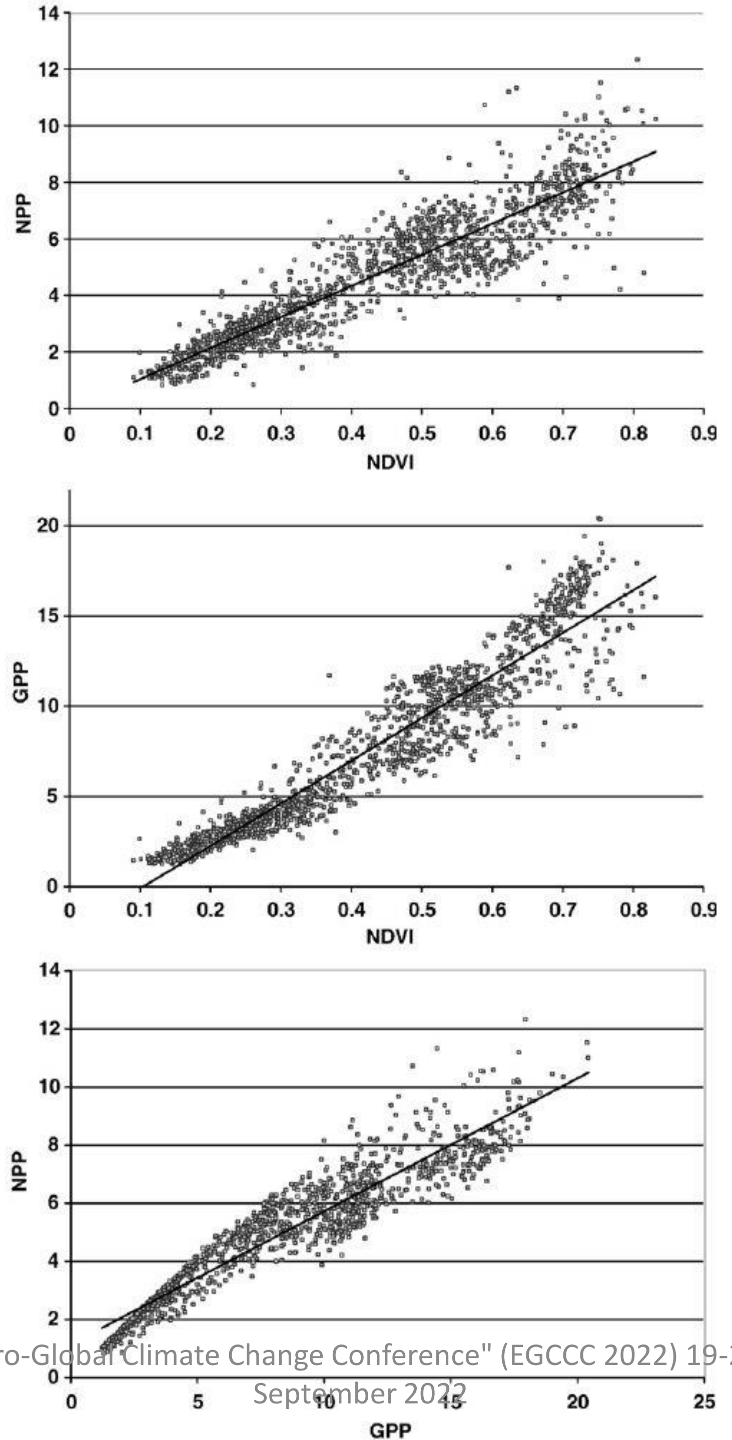

Evaluating the species energy relationship with the newest measures of ecosystem energy: NDVI versus MODIS primary production (DOI:10.1016/j.rse.2008.04.012)

Linda Philips; Andrew Hansen ; Curtis H Flather

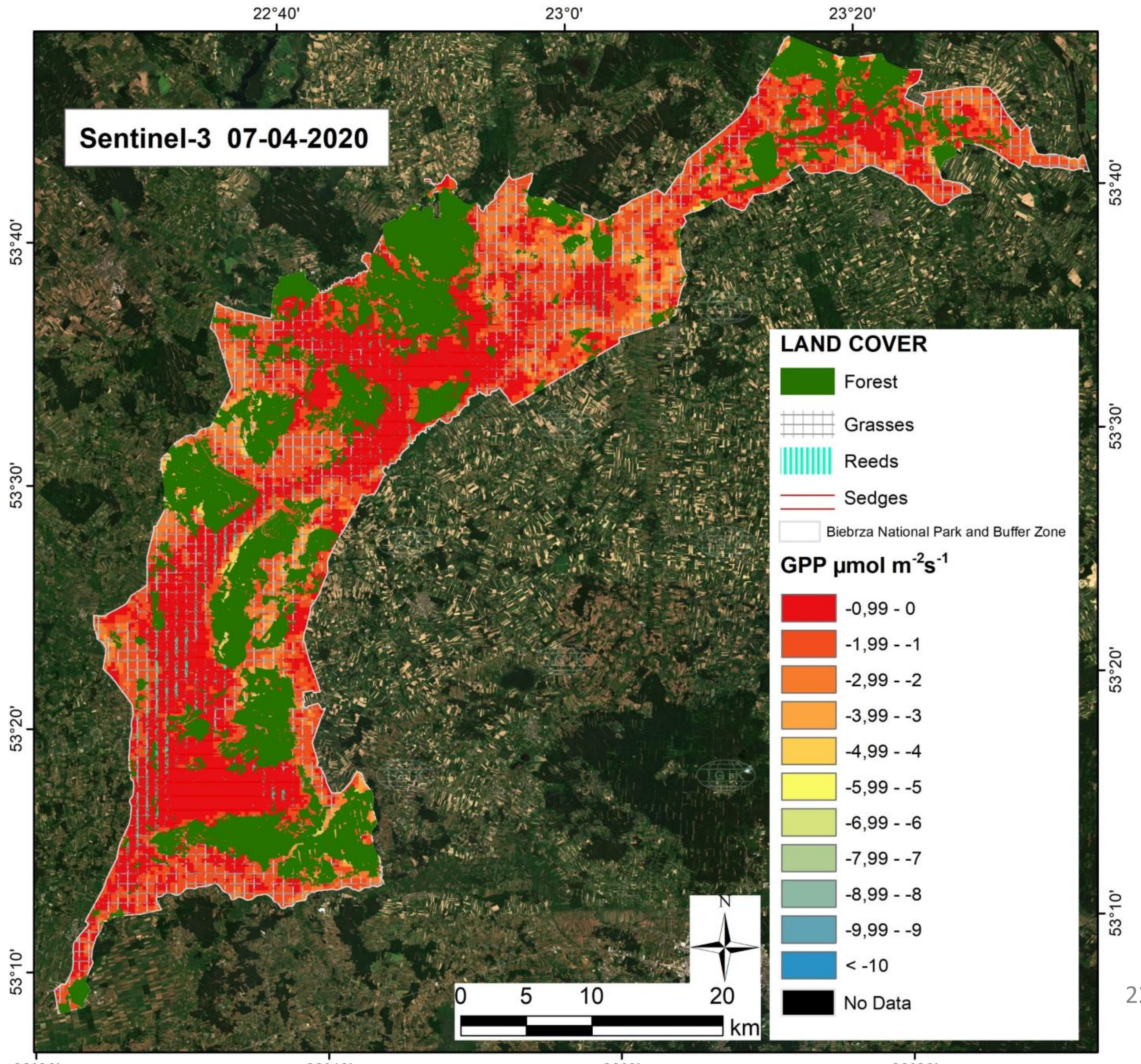
Sentinel-3 07-04-2020
22°40'
23°0'
23°20'
53°40'
53°30'
53°20'
53°10'
LAND COVER
Forest
Grasses
Reeds
Sedges
Biebrza National Park and Buffer Zone
GPP µmol m-2s-1
-0,99 - 0
-1,99 - -1
-2,99 - -2
-3,99 - -3
-4,99 - -4
-5,99 - -5
-6,99 - -6
-7,99 - -7
-8,99 - -8
-9,99 - -9
< -10
No Data
N
0 5 10 20
km

22) 19-20

May 2020 05.21

GPP modeled from Sentinel3 satellite data

2020 08 28

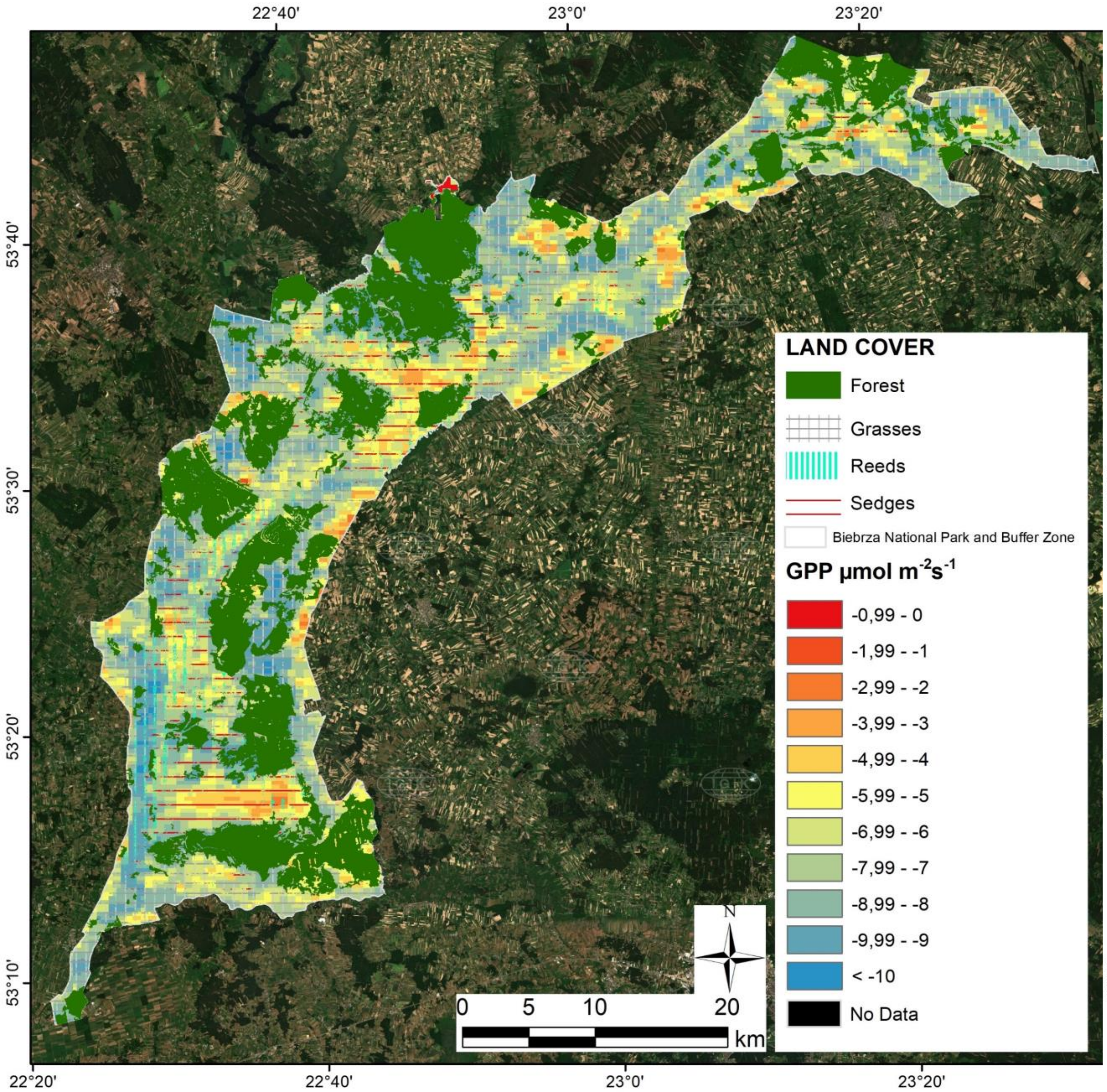

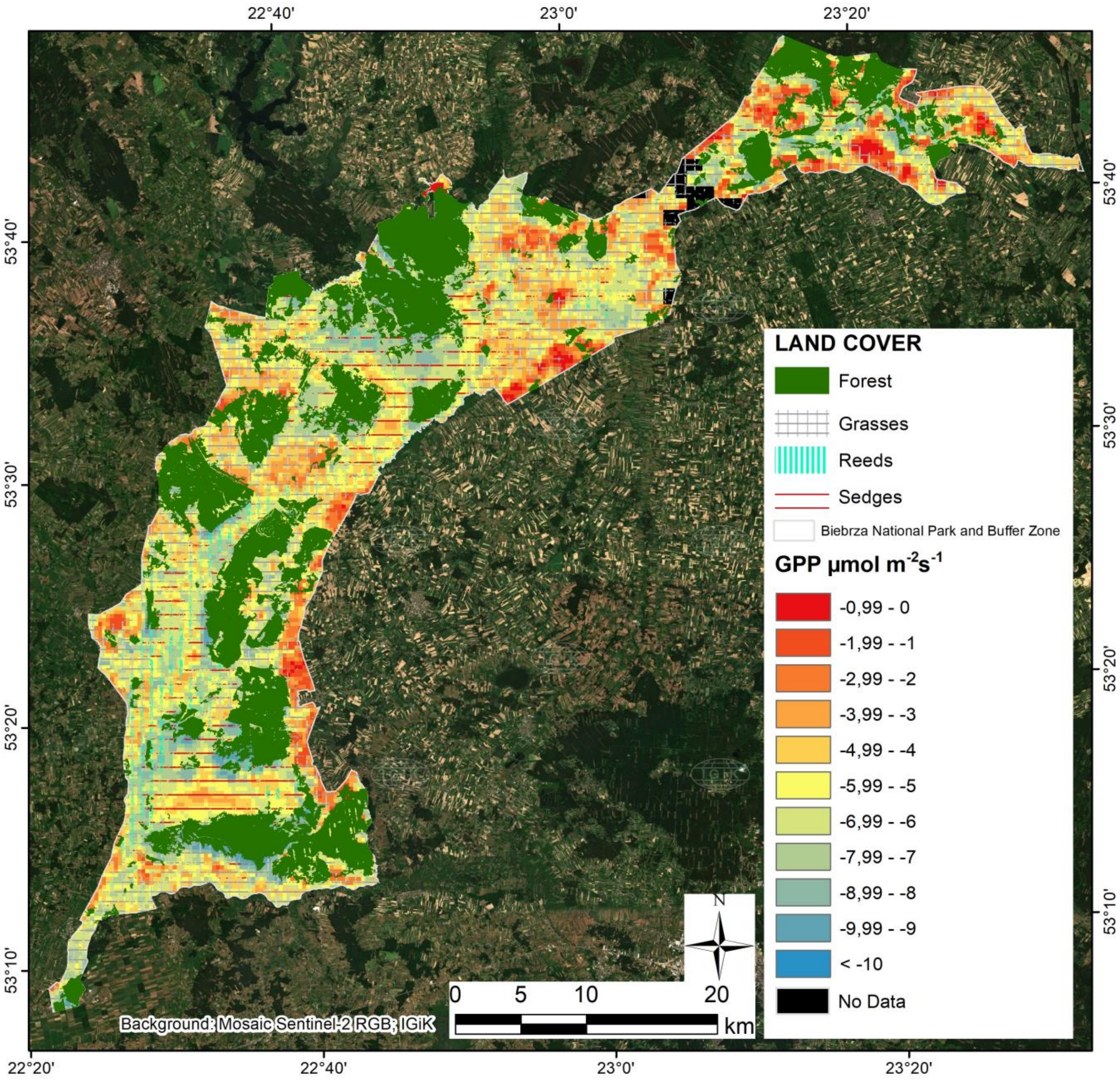

(Ts –Ta) as the drought – humidity indicator

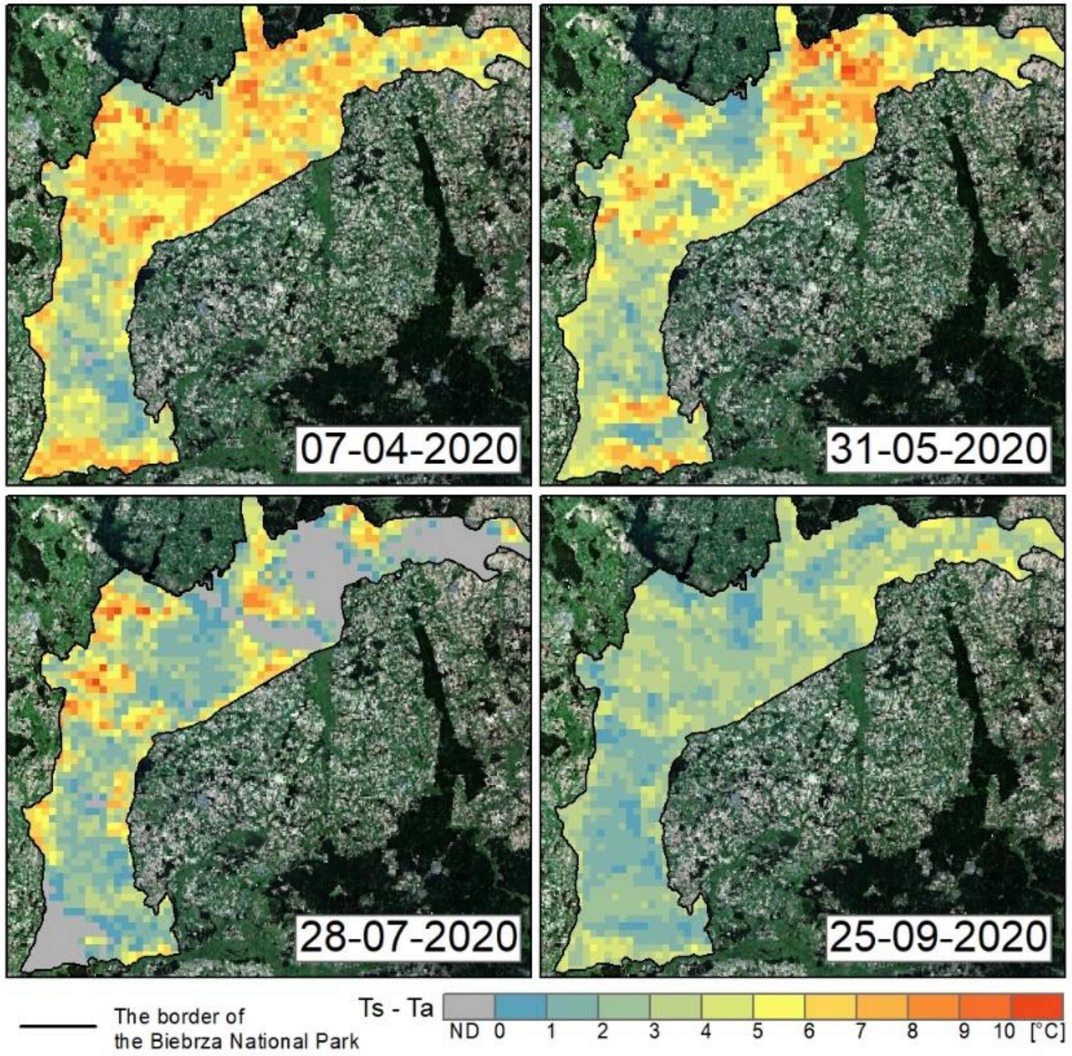

NDVI representing the biomass

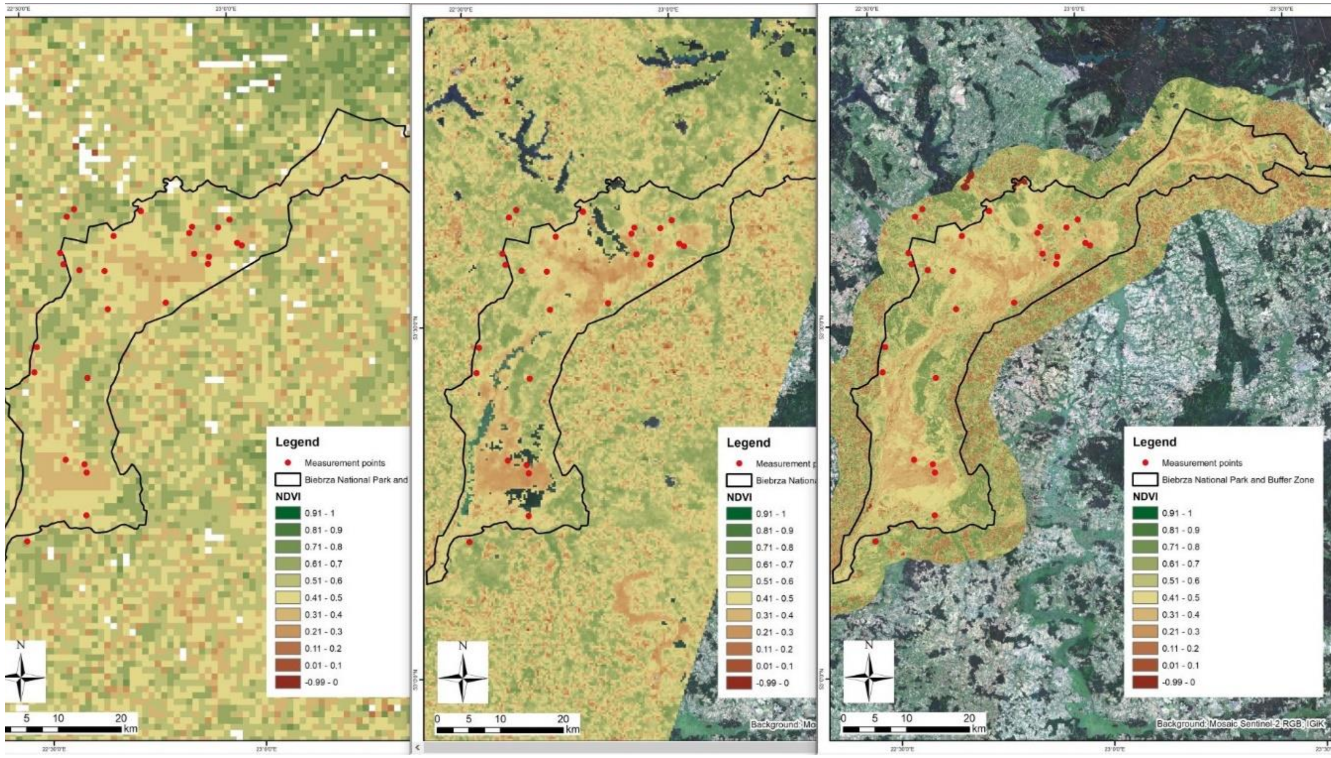

Ewapotranspiracja obliczona ze strumienia utajonego LE maps – Biebrza test site – Landsat based LST
Obliczono Dzienne Wartości Ewapotranspiracji

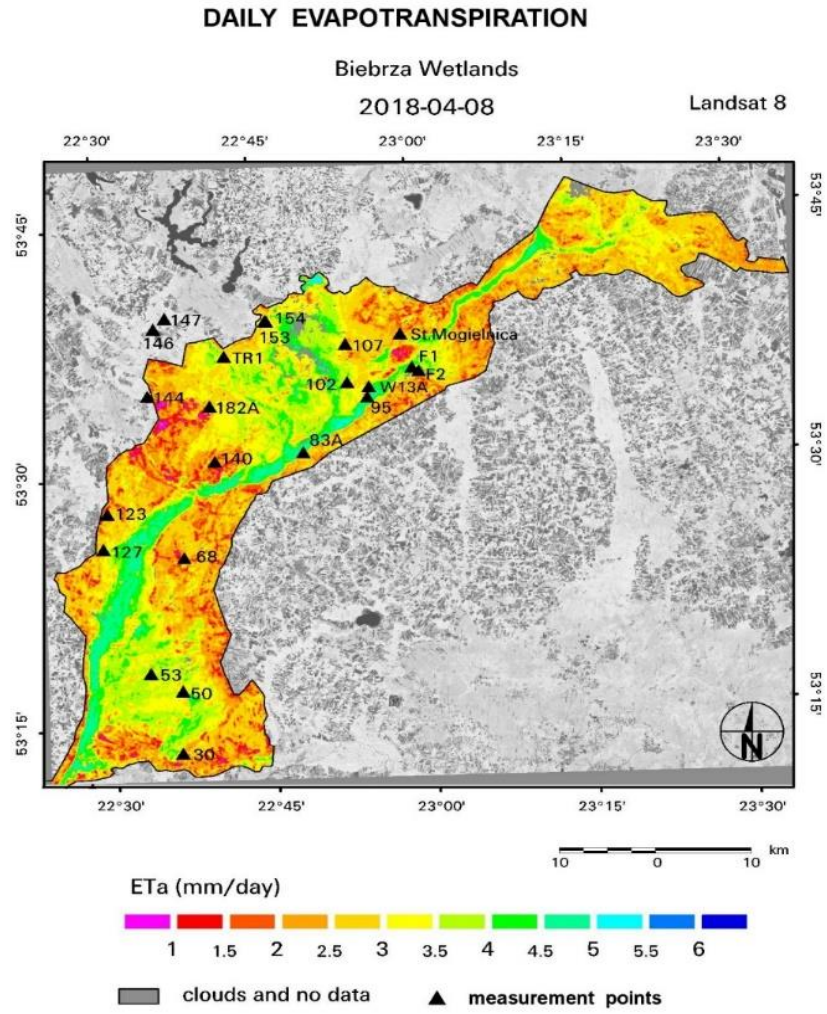

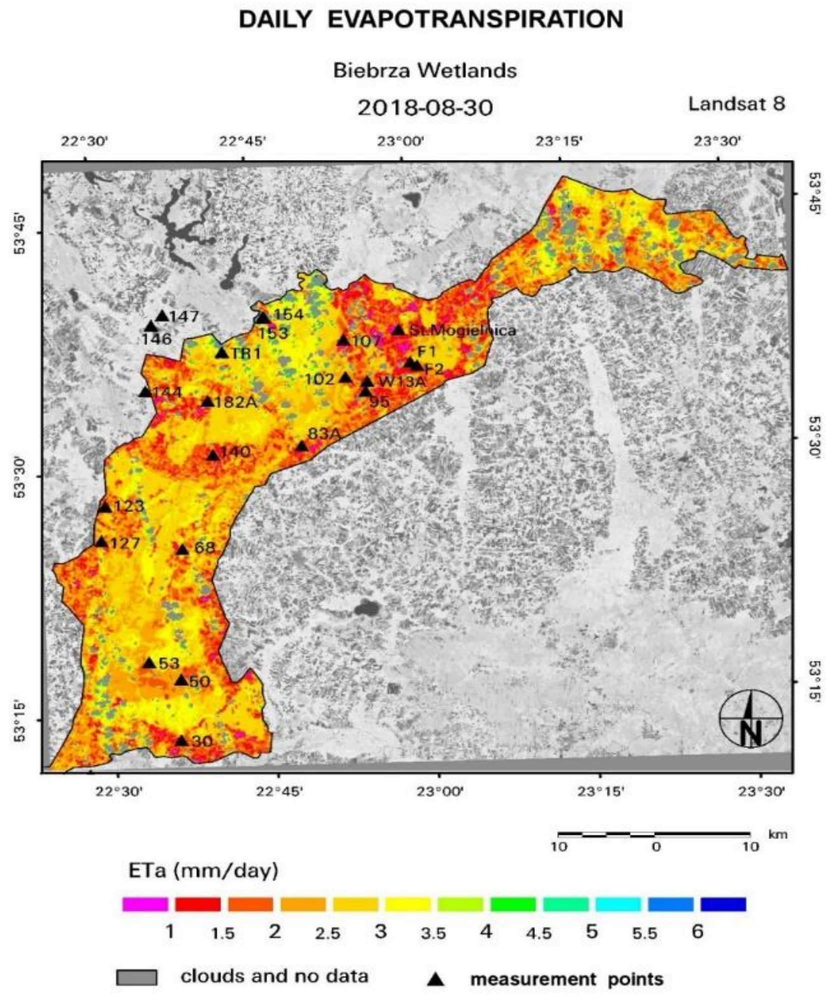

Biebrza wetlands Area

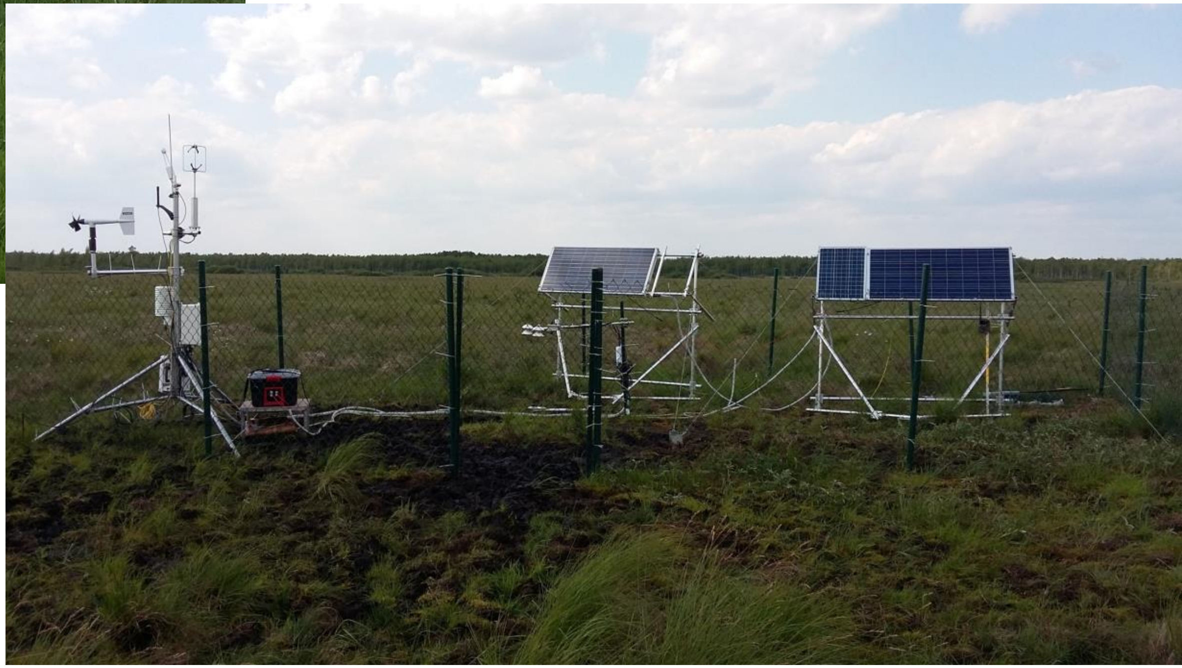

Models for daily values for Gross Primary Production - GPP

Satellite	Formula	R[1]	N[2]
Terra MODIS	$\overline{GPP}_{day} = -0.37 \cdot \exp(3.87 \cdot NDVI_{MODIS} + 0.000204 \cdot APAR)$	0.70	78
	$\overline{GPP}_{11:00} = -1.66 \cdot \exp(2.87 \cdot NDVI_{MODIS} + 0.0008 \cdot LE_{MODIS})$	0.55	107
	$\overline{GPP}_{day} = -2.72 \cdot \exp(0.13 \cdot LAI_{S2} + 0.089 \cdot Ead_{MODIS})$	0.57	73
Sentinel 2	$\overline{GPP}_{day} = -0.37 \cdot exp(3.15 \cdot NDVI_{S2} + 1.71 \cdot NDII_{S2})$	0.78	60
Sentinel 3	$\overline{GPP}_{day} = -0.16 \cdot \exp(4.39 \cdot NDVI_{S3} - 0.004 \cdot (T_s - T_a)^2)$	0.80	68
	$\overline{GPP}_{09:00} = -0.12 \cdot \exp(4.87 \cdot NDVI_{S3} + 0.0008 \cdot LE_{S3})$	0.73	66

The Climate Change reflects changes of air temperature, increases changes of the difference between surface and air temperature, diminishes the vegetation vigor and biomass.

Carbon dioxide emissions from peatland drainage, fires and exploitation are estimated to be the equivalent to at least 3,000 million tons per year. Climate changes induce decrease of precipitation and growth of air temperature what influences the exchange of the gases between the surface and atmosphere and lowers the soil moisture, what results in release of CO_2 to the atmosphere.

Wetlands as the residual of peat due to the changes drain water and change the environment causing succession of other vegetation, which is alient to the environment

Lessening Water shortages

Water security

- Water supply monitoring and management
- Water quality simulation & data alerts
- Self-adaptive water filtration
- Asset maintenance on critical water and wastewater expenditures

- Harmful algal blooms detection and monitoring
- Streamflow forecasting
- Automated flood centred infrastructure

- Drought prediction
- Simulations for drought planning
- Drought impact assessments

- Residential water use monitoring and management
- Optimisation of industrial water use
- Predictive maintenance of water plants
- Early warning system for water infrastructure
- Detect underground leaks in potable water supply systems
- Smart meters in homes

- Drones and AI for real-time monitoring of river quality
- Ensuring adequate sanitation of water reserves
- Real-time monitoring and management of household water supply

Mitigation of Climate Changes

Climate change

- Optimised energy system forecasting
- Smart grids for electricity use
- Predict solar flares for protecting power grids
- Renewable energy plant assessments
- Optimised decentralised & peer-to-peer renewable energy systems
- Optimised virtual power plants

- Smart traffic light & parking systems for urban mobility management
- Optimised sustainable building design
- Energy-efficient building management systems
- Auditory responsive lighting & heating
- Optimised urban-level energy generation and use
- Analytics & automation for smart urban planning

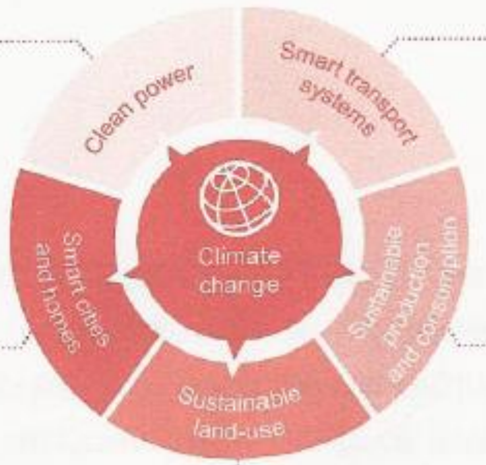

- On-demand shared transport mobility
- AI-enabled electric cars
- Autonomous vehicles for efficient transport
- Vehicle to infrastructure communication and optimisation
- Optimised traffic flows
- Integrated cost-efficient transport systems
- Demand-response charging infrastructure

- Supply chain monitoring and transparency
- Active optimisation of industrial machinery & manufacturing
- Digital twins for lifespan performance optimisation
- Smarter fresh-food replenishment
- Smart recycling systems
- Integrated municipal & industrial waste management

- Early crop yield prediction
- Precision agriculture & nutrition
- Hyper-local weather forecasting for crop management
- Early detection of crop issues
- Automated & enhanced land-use change detection for avoided deforestation
- Monitoring health & well-being in livestock farming